Discharge current modes of high power impulse magnetron sputtering

Zhongzhen Wu, Shu Xiao, Zhengyong Ma, Suihan Cui, Shunping Ji, Xiubo Tian, Ricky K. Y. Fu, Paul K. Chu, and Feng Pan

Citation: AIP Advances **5**, 097178 (2015); doi: 10.1063/1.4932135
View online: http://dx.doi.org/10.1063/1.4932135
View Table of Contents: http://scitation.aip.org/content/aip/journal/adva/5/9?ver=pdfcov
Published by the AIP Publishing

Discharge current modes of high power impulse magnetron sputtering

Zhongzhen Wu,[1,a] Shu Xiao,[1] Zhengyong Ma,[1] Suihan Cui,[1] Shunping Ji,[1] Xiubo Tian,[2] Ricky K. Y. Fu,[3] Paul K. Chu,[3] and Feng Pan[1]
[1]*School of Advanced Materials, Shenzhen Graduate School, Peking University, Shenzhen 518055, China*
[2]*State Key Laboratory of Advanced Welding and Joining, Harbin Institute of Technology, Harbin 150001, China*
[3]*Department of Physics and Materials Science, City University of Hong Kong, Tat Chee Avenue, Kowloon, Hong Kong, China*

(Received 28 May 2015; accepted 16 September 2015; published online 28 September 2015)

Based on the production and disappearance of ions and electrons in the high power impulse magnetron sputtering plasma near the target, the expression of the discharge current is derived. Depending on the slope, six possible modes are deduced for the discharge current and the feasibility of each mode is discussed. The discharge parameters and target properties are simplified into the discharge voltage, sputtering yield, and ionization energy which mainly affect the discharge plasma. The relationship between these factors and the discharge current modes is also investigated. [http://dx.doi.org/10.1063/1.4932135]

High power impulse magnetron sputtering (HiPIMS) is a hot topic in the field of physical vapor deposition (PVD) because of high ionization of the sputtered materials.[1] The ionized particles in HiPIMS enhance ion bombardment and implantation energy with the assistance of a bias to yield epitaxial growth, excellent film adhesion, and good coating density.[2,3] As a result of these advantages, HiPIMS is very attractive to the deposition of hard coatings,[4–6] decorative coatings, biologic coatings[7] and photoelectric coatings.[8] However, the discharge of different materials does not have the same ionization and stability as DC magnetron sputtering or cathodic arc ion plating.[9–11] For example, ionization of Cu is more than 90% and the discharge is stable, but frequent arcing is observed from C in HiPIMS and ionization is quite low. The current waveforms also vary with different target materials,[12] and even for the same target material, they are distinct at different discharge voltages.[13] Although an extra magnetron filed or Ne can be used to increase the stability and ionization of the C discharge in HiPIMS,[14,15] it is difficult to optimize the process after changing the target materials. Hence, a general discharge model of HiPIMS and better understanding of the relationship between the discharge and deposition parameters are important in order to fully exploit the advantages of the technique. In this respect, most research activities have focused on the experimental investigation of the discharge currents of different materials,[16] but the theoretical assessment is relatively scarce. Herein, we present a theoretical approach for the discharge current in HiPIMS and based on the evolution of the current slope, six waveforms are deduced and the feasibility of each mode is discussed.

The discharge current of the HiPIMS discharge is produced mainly by two mechanisms: ions attracted to the target by the negative potential at the target from the plasma nearby and secondary electrons emitted from the ion bombardments.[17,18] Here, $n^i(t)$ is assumed to be the total ion density in the plasma at any time t during the impulse, β is the percentage of ions attracted back to the target,

[a]Corresponding author. Tel/Fax: 86-755-21537403. *E-mail address:* wuzz@pkusz.edu.cn (Z. Z. Wu)

and γ is the average secondary electrons emission coefficient of the target. The discharge current I (t) at time t is given by

$$I(t) = \int n^i(t)\beta(1+\gamma)\,dA \tag{1}$$

where A is the area of the target. The evolution of the ion density is determined by ion production as well as disappearance. In the HiPIMS discharge, ion production is attributed to the ionization of atoms sputtered from the target and the gas introduced to the plasma. Ions disappear by two ways: back attraction due to the negative target potential and ion diffusion and recombination with electrons in the plasma or on the vacuum chamber wall. We assume that all the particles sputtered from the target and gas entered the plasma are neutral atoms, and the diffusion and recombination possibilities of both gas ions and metallic ions which don't return to the target are equal. Hence, in a short time, Δt, the ion density back to the target Δn_T^i (all these ions contribute to the sputtering) is expressed by

$$\Delta n_T^i = n^i(t)\,\beta\,\Delta t \tag{2}$$

and the lost ions Δn_D^i is

$$\Delta n_D^i = n^i(t)\,(1-\beta)\,\varepsilon\,\Delta t \tag{3}$$

where ε is the disappearance rate, that is, the ratio of the ions lost by diffusion and recombination to the ions not returning to the target.

The disappearing electrons are equal to the lost ions because electrons travel much faster than ions and the plasma is electroneutral. That is,

$$\Delta n_{loss}^e = \Delta n_{loss}^i = \Delta n_T^i + \Delta n_D^i \tag{4}$$

Production of electrons stems from secondary electrons emission during sputtering and collisions in the plasma. The density of the emitted secondary electrons at time Δt can be written as:

$$\Delta n_{emit1}^e = \Delta n_T^i \gamma = n^i(t)\,\beta\,\gamma\,\Delta t \tag{5}$$

α is assumed to be the average number of electrons produced during the collisions and hence, the density of this portion of the electrons at Δt can be expressed as

$$\Delta n_{emit2}^e = n^i(t)\,\alpha\,\Delta t \tag{6}$$

The density of the total electrons Δn_{emit}^e in the plasma in Δt is the sum:

$$\Delta n_{emit}^e = \Delta n_{emit1}^e + \Delta n_{emit2}^e = n^i(t)\,\beta\gamma\Delta t + n^i(t)\,\alpha\,\Delta t \tag{7}$$

Owing to the electroneutrality, the change of the plasma density in the considered area at Δt is equal to that of the ions density and that of the electron density. That is,

$$dn(t) = dn^i(t) = dn^e(t) = \Delta n_{emit}^e - \Delta n_{loss}^e = \Delta n_{emit}^e - \Delta n_T^i - \Delta n_D^i \tag{8}$$

Equation (1) can be written as:

$$\frac{dI(t)}{dt} \propto \frac{dn^i(t)}{dt} = n^i(t)\,\beta\left[\gamma + \frac{\alpha}{\beta} - 1 - \left(\frac{1}{\beta} - 1\right)\varepsilon\right] \tag{9}$$

In the equation, the total ion density is positive and the ratio of the ion returning to the target β satisfies $0 < \beta < 1$. The evolution of the discharge current at any moment (the slope of the discharge current versus time plot) depends on a constant Φ that is determined by the four parameters: γ, α, ε and β.

$$\Phi = \gamma + \frac{\alpha}{\beta} - \left[1 - \varepsilon\left(1 - \frac{1}{\beta}\right)\right] \tag{10}$$

In the HiPIMS discharge, the four parameters change with time and consequently affect the waveform of the discharge current. As shown in equation (10), the discharge current increase with time for $\Phi > 0$, decrease for $\Phi < 0$, and has extreme values for $\Phi = 0$.

Considering HiPIMS in the constant-voltage mode, the ratio of ions back to the target β is constant throughout the impulse. Mainly two factors, ion energy and mean free path, determine the average number of electrons produced in the collisions (mainly ion-electron and atom-electron collisions according to the cross section) in the plasma.[19] The former is related to discharge voltage and therefore, it will stay the same in the constant-voltage mode. The later depends on pressure (total pressure in a chamber) which is normally unchanged in the HiPIMS process. Therefore, the average number of electrons produced in the collision α can be treated as a constant.

L. Poucques et al. have shown that the ion diffusion behavior in the plasma of HiPIMS follows the ambipolar diffusion theory in which the disappearance rate ε depends on the plasma density, temperature, and pressure.[20] Here, pressure is a total pressure in a chamber and it is constant. At the beginning of the discharge, the plasma develops quickly but the temperature is the same in a short time. Consequently, the plasma density dictates the disappearance rate ε. When the discharge is intense and stable, the change in the plasma density becomes inconspicuous and the temperature has enough time to evolve. Therefore, the disappearance rate ε at this time is determined by and proportional to the temperature.

The average secondary electron emission coefficient of the target bombarded by ions, γ, is determined by the composition of the plasma as follows:

$$\gamma = \frac{\sum_{i=1}^{n} n_g^i \gamma_g^i + \sum_{i=1}^{n} n_m^i \gamma_m^i}{\sum_{i=1}^{n} n_g^i + \sum_{i=1}^{n} n_m^i} \tag{11}$$

where i is charge of an ion returning to the target, n_g^i, n_m^i are the density of the gas ions and the metal ions back to the target with charge i, respectively, γ_g^i, and γ_m^i are the secondary electron emission coefficient of the target bombarded by gas ions and metal ions with charge i, respectively.

Two kinds secondary electron emission, kinetic emission and potential emission, occur when ions impinge the target surface.[21] Generally, kinetic emission dominates when the energy of the incident ion is over 300 eV/amu. However, in HiPIMS, the energy of the incident ion is much lower than the emission threshold, suggesting that kinetic emission is rare and can be neglected. Herein, we consider only potential emission with a low threshold produced mainly by collisions between the incident ions and the target surface. The following empirical formula is used to illustrate the potential emission of the secondary electrons γ_{se}:[22]

$$\gamma_{se} = 0.032\left(0.78E_{pot} - 2\phi\right) \tag{12}$$

Equation (12) suggests that secondary electron emission coefficient is determined by the ionization energy of the incident ions E_{pot} and work function of the sputtering materials ϕ. Tab. I shows the ionization energy and work functions of some common materials.[12,23] The secondary electron emission coefficient of metal ions is normally smaller than that of Ar ions with the same charge and the secondary electron emission coefficients increase with the charge state. This suggests that the average secondary electron emission coefficient γ depends on the composition and charge state of the plasma and the gas ions and multiply charged ions increase the average secondary electron coefficient.

As shown in equation (10), only two of the four parameters (ε and γ) change with discharge time in the process of HiPIMS. For simplicity, we assume

$$\lambda = \gamma + \frac{\alpha}{\beta} \tag{13}$$

$$\eta = 1 - \varepsilon\left(1 - \frac{1}{\beta}\right) \tag{14}$$

where λ depends on γ and η depends on ε. We can deduce the slope of the discharge current waveform (Φ) according to the evolution of η and λ and consequently all the possible discharge current modes with time at a certain discharge voltage.

For simplicity, we only discuss the discharge in a single impulse without considering the interaction of the consecutive impulses and the impulse is long enough for evolution of the discharge

current, otherwise, the discharge current will be interrupted when the impulse ends. In this case, the discharge current waveform is a segment of that of the long impulse or there is only a small change which is not discussed here. In a long single impulse, the discharge starts after the initiation of the discharge voltage when the voltage is larger than the discharge threshold. Many collisions occur in the beginning and the production of electrons is faster than disappearance and recombination. Hence,

$$\lambda >> \eta \tag{15}$$

In equation (10) $\Phi > 0$, suggesting that the discharge current begins with a sharp increase after the initial of the voltage impulse. In the beginning, the gas (Ar) is ionized first[23] and almost all the ions in the plasma are gas ions and the sputtering ions are only Ar. According to equations (11), (12) and Tab. I, the secondary electron emission coefficient γ_g^1 is contributed by Ar^+. At this time, diffusion and recombination have not started and in equation (15), $\eta = 1$.

Sputtering of metal target happens when the Ar ions bombard the target. The sputtered metal atoms become ionized when colliding with other particles in the plasma. Once ionized, some of the metal ions will be attracted back to the target by the negative target potential thus participating in sputtering again in the process termed self-sputtering.[24] Afterwards, more metal particles are introduced to the plasma and out-number the original gas ions gradually. According to equation (11), the average secondary electron emission coefficient decreases with the increasing discharge intensity. At the same time, heat is generated with increasing discharge intensity. The plasma temperature rises and induces rarefaction effect in the plasma to increase of the disappearance rate ε. Based on equation (10), Φ decreases, and it will continue until a balance between the production and disappearance of metal ions in the plasma is reached. In the equilibrium stage, the plasma density and composition are almost constant and the gas ions and metal ions exist in a constant ratio determined by the sputtering yield,[25] and the average secondary electron emission coefficient γ does not change until the end of the impulse. However, if the applied discharge voltage is larger enough, the larger plasma density and more collisions produce highly charged ions[26,27] and regardless of whether they are gas ions or metal ions, will increase the average secondary electron emission coefficient γ and the increase is positively correlated to the ionization energy.

As illustrated in the analysis above, the evolution of the discharge current slope is determined by three conditions: (1) whether $\Phi = 0$ or the inflexion point occurs in the sputtering process, (2) when the composition balance of the plasma is achieved in the sputtering process, and (3) whether a large number of highly charged ions appears after the plasma balance. According to equation (10) and these three conditions, six kinds of possible waveforms of the HiPIMS discharge current can be deduced from the evolution of the slope.

Firstly, if $\lambda \geq \eta$ is satisfied throughout the impulse, highly ionized ions must be produced to increase γ again in the later discharge to keep λ larger than η because γ decreases with sputtering and η increases with the discharge intensity and sputtering in the initial of the impulse. According to equation (10), $\Phi \geq 0$, the discharge current increases monotonically and the extreme happens at the end of the impulse.

Considering the composition of the plasma and if the sputtering rate is low, the discharge is weak and the composition of the plasma is dominated by gas ions which improve γ sharply by high

TABLE I. Work function and first and second ionization energies for selected materials.

Materials	Φ (eV)	$E_{0\to1}$ (eV)	$E_{1\to2}$ (eV)
Ar	n/a	15.76	27.63
Ti	4.3	6.82	13.58
Cu	4.9	7.73	20.29
Cr	4.5	6.77	16.49
Nb	4.2	7.67	14.32
W	4.55	7.98	17.62
Al	4.28	5.99	18.83
C	4.53	11.26	24.38
Au	5.3	9.23	20.50

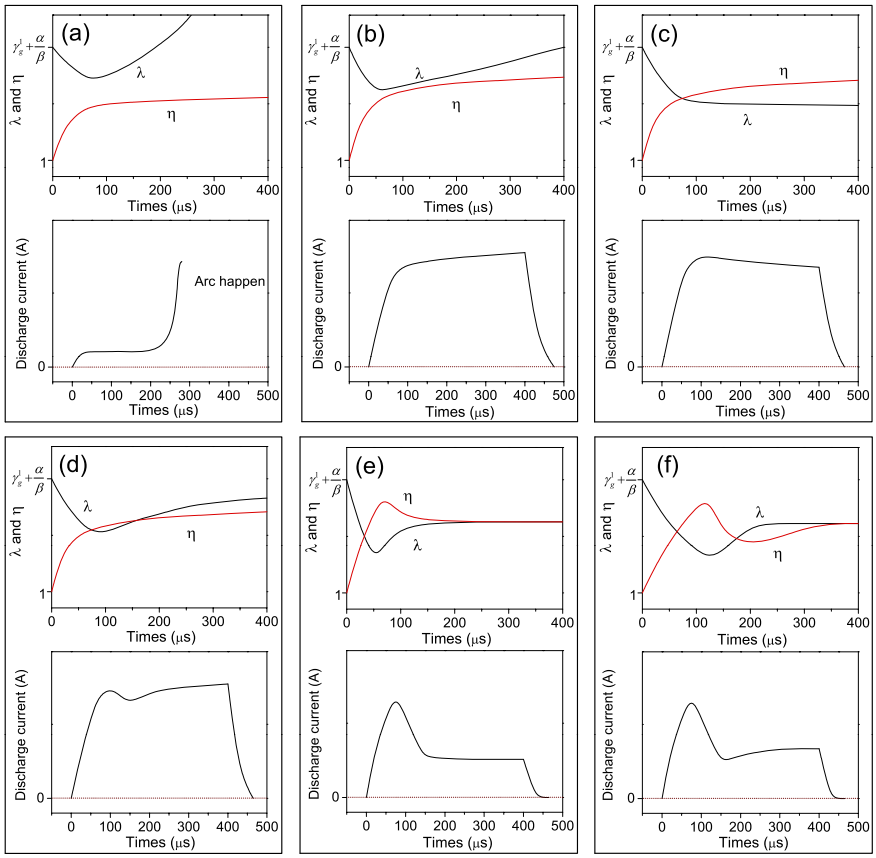

FIG. 1. Evolutions of λ, η, and possible modes of HiPIMS discharge current waveforms (a) Mode I; (b) Mode II; (c) Mode III; (d) Mode IV; (e) Mode V; (f) Mode VI.

ionization. Therefore, the beginning discharge current is small but it increases sharply when highly ionized ions are produced at high voltage. Arcing always occurs due to the uncontrollable increase in the discharge current.[11] The schematic evolution of λ, η and the discharge current are shown in Fig. 1(a) and termed Mode I.

If the sputtering rate is high, the discharge is intense from the beginning to the end of the impulse and the plasma is dominated by metal ions swiftly. In this way, the discharge current increases rapidly to a high level until a discharge equilibrium. Highly charged ions are necessary for the condition of $\lambda \geq \eta$ but the improvement by metal ions on γ is gentle compared to that of gas ions with increasing charge number. Consequently, the increase in the discharge current is gentle after the balance and it is designated as Mode II in Fig. 1(b).

If $\Phi = 0$ happens during the impulses together with decrease in the average secondary electron emission coefficient γ and increase in the loss rate ε, a maximum appears in the discharge current waveform after the initial sharp rise. After the inflexion point, the discharge current starts to decrease corresponding to $\Phi < 0$ in equation (10). In this case, if the sputtering rate is high enough, the discharge balance occurs before $\Phi = 0$. The discharge is intense and the equilibrium plasma is dominated by metal ions as shown in Fig. 1(b). The discharge current also increases sharply at the beginning of the impulse and there is a maximum later. If no highly charged metal ion appears in the later HiPIMS process, γ does not change anymore after equilibrium. As a result, the discharge current diminishes gently as the plasma temperature increasing gradually because of rarefaction effect. The schematic evolution of λ, η and the discharge current waveform with time are shown in Fig. 1(c) and is termed Mode III.

Another situation is that the ionization energy of the target materials is low enough so that the sputtering metal ions can be ionized further in the later HiPIMS process and γ will increase again.

Generally, the increase rate of λ is larger than that of η, $\Phi = 0$ will appear again resulting in another inflection point (minimum) in the discharge current waveform. The discharge current should increase again after the minimum until the end of the impulse and this is Mode IV as shown in Fig. 1(d).

If the sputtering rate is very low and $\Phi = 0$ occurs before equilibrium, the replacement of gas ion by sputtered metal ions is ongoing when the maximum appears. This feature induces a sustained and sharp decrease in γ and consequently, the discharge current diminishes after the maximum until the equilibrium is established. In equilibrium, the plasma is mixed with metal ions and gas ions with a certain ratio and the discharge intensity is weak resulting in no apparent change in the temperature. Therefore, if no highly charged ions are produced, the discharge current will show a plateau after the equilibrium until the end of the impulse, as shown in Fig. 1(e) which is called Mode V.

Although uncommon, highly charged ions still can be generated in the later stage of discharge after equilibrium. If so, the discharge current will increase again with increasing γ and then the plasma density will increase slightly to achieve another balance, as shown by Mode VI in Fig. 1(f).

As aforementioned, the average secondary electron emission coefficient in the plasma depends on the replacement rate gas ions by metal ions and production of highly charged ions. The former dictates when equilibrium is achieved and the later determines the increase of γ after the initial decrease at the beginning of the impulse. In HiPIMS, the sputtering rate depends on the sputtering yield of the target materials Y and the applied discharge voltage U,[28] and the production of highly charged ions is related to the ionization energy of particles I_{Metal} and the applied discharge voltage U. The plasma density and temperature which determine the disappearance rate ε are related to the applied discharge voltage and time. However, ε increases monotonically with discharge time. In summary, the slope Φ which shows the evolution tendency is contributed by only three parameters: the applied discharge voltage U, the sputtering yield of target materials Y, and the ionization energy of the particles I_{Metal}. Later, we will establish the relationship between these three parameters and the six modes of discharge currents.

Concerning the sputtering process in HiPIMS, previous researchers usually use Π_{ss} to characterize self-sputtering[12,29] and three intervals of Π_{ss} are obtained and they almost correspond to the three conditions of the plasma composition equilibrium.[13,16,22] That is, for $\Pi_{ss} \geq 1$, the balance happens before the peak of the discharge current as shown in Fig. 1(b), 1(c) and 1(d). For $0.1 < \Pi_{ss} < 1$, the balance happens after the peak of the discharge current as shown in Fig. 1(e) and 1(f). For $\Pi_{ss} \leq 0.1$, no balance occurs in the whole impulse as shown in Fig. 1(a). For simplicity, we divide the sputtering yield, ionization energy, and discharge voltage into six sections as shown in Fig. 2, in which ADF'F is the interface with $\Pi_{ss} = 0.1$, BCE'E is the interface with $\Pi_{ss} = 1$, and BCE'B and BCF'E are the interface of highly charged metal ions determined by the ionization energy and discharge voltage. Each section corresponds to one of the possible forms of the discharge current, for instance, the sputtering yield being very low in ADD'A'FF' corresponding to mode I in Fig. 1(a), the sputtering yield being very high but the ionization energy being low in B'C'E'G corresponding to mode II in Fig. 1(b), the sputtering yield being high enough and ionization energy being high in CBB'E'E corresponding to mode III in Fig. 1(c), the sputtering yield being high enough but the ionization energy being low in BCGE'B' corresponding to mode IV in Fig. 1(d), the sputtering yield being low but the ionized energy being high in CBEE'F' corresponding to mode V in Fig. 1(e), and both the sputtering yield and ionization energy being low in ABCDF'FE corresponding to mode VI in Fig. 1(f).

Modes II, III and IV are obtained from target materials with high sputtering yield and the discharge is stable without hysteresis effects during reactive magnetron sputtering.[30] Therefore, these three forms are ideal for HiPIMS. In Mode V and VI, the sputtering yield of the target materials is low and the discharge is weak but stable. It can generally be used in depositions but the process is sensitive to the reactive gases[31] and it is difficult to achieve a uniform and stable film. Mode I corresponds to materials with a very low sputtering yield. The discharge is weak and unstable even at a high voltage and continuous arcing may occur. Hence, in this mode, other improvements should be made.[14,15]

In summary, the expression for the HiPIMS discharge current is developed theoretically and there are six possible discharge current modes according to the evolution of the slope. The discharge parameters and the target materials properties are determined by discharge voltage, sputtering yield,

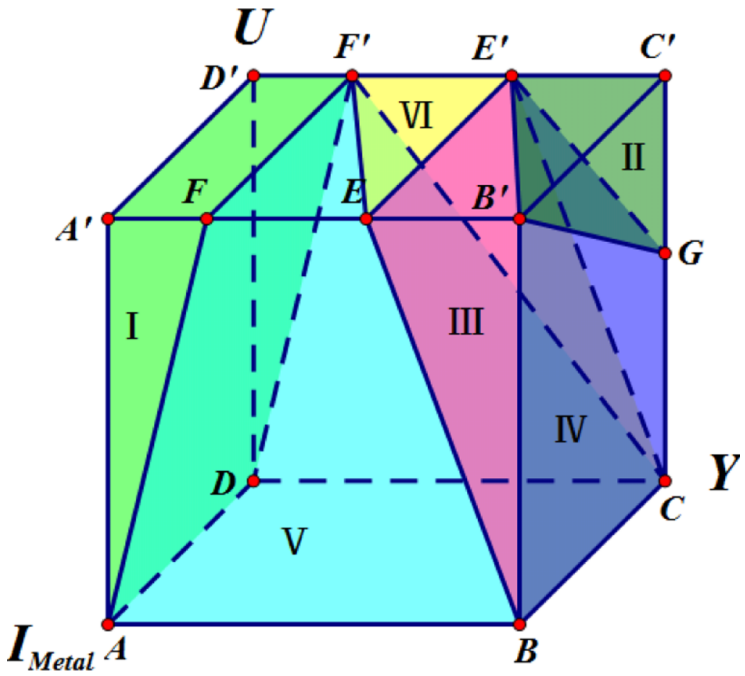

FIG. 2. Relationship between each discharge current modes and the three deposition parameters: sputtering yield, ionization energy, and discharge voltage.

and ionization energy, which affect the discharge plasma. The relationship of each discharge current mode is established in order to predict the discharge behavior.

This work was financially supported jointly by Natural Science Foundation of China (No. 51301004, U1330110), Shenzhen Science and Technology Research Grant Guangdong - Hong Kong Technology Cooperation Funding (SGLH20120928095706623 and GHP/015/12SZ), and City University of Hong Kong Strategic Research Grant (SRG) No. 7004188.

[1] V. Kouznetsov, K. Macák, J. M. Schneider, U. Helmersson, and I. Petrov, Surf. Coat. Technol. **122**, 290 (1999).
[2] A.P. Ehiasarian, W.-D. Munz, L. Hultman, U. Helmersson, and I. Petrov, Surf. Coat. Technol. **163-164**, 267 (2003).
[3] A.P. Ehiasarian, J.G. Wen, and I. Petrov, J. Appl. Phys. **101**, 054301 (2007).
[4] P.E. Hovsepian, A.P. Ehiasarian, R. Braun, J. Walker, and H. Du, Surf. Coat. Technol. **204**, 2702 (2010).
[5] K. Bobzin, N. Bagcivan, M. Ewering, R.H. Brugnara, and S. Theiß, Surf. Coat. Technol. **205**, 2887 (2011).
[6] S. Yang, X. Li, K.E. Cooke, and D.G. Teer, Appl. Surf. Sci. **258**, 2062 (2012).
[7] O. Baghriche, A.P. Ehiasarian, E. Kusiak-Nejman, C. Pulgarin, R. Sanjines, A.W. Morawski, and J. Kiwi, J. Photochem. Photobio. A: Chem. **227**, 11 (2012).
[8] S. Kment, Z. Hubicka, J. Krysa, D. Sekora, M. Zlamal, J. Olejnicek, M. Cada, P. Ksirova, Z. Remes, P. Schmuki, E. Schubert, and R. Zboril, Appl. Catal. B: Env. **165**, 344 (2015).
[9] K. Sarakinos, J. Alami, and S. Konstantinidis, Surf. Coat. Technol. **204**, 1661 (2010).
[10] E. Oks and A. Anders, J. Appl. Phys. **105**, 093304 (2009).
[11] M. Lattemann, B. Abendroth, A. Moafi, D.G. McCulloch, and D.R. McKenzie, Diamond Relat. Mater. **20**, 68 (2011).
[12] A. Anders, J. Andersson, and A. Ehiasarian, J. Appl. Phys. **102**, 113303 (2007).
[13] C. Huo, D. Lundin, M. A. Raadu, A. Anders, J. T. Gudmundsson, and N. Brenning, Plasma Sources Sci. Technol. **23**, 025017 (2014).
[14] J. Čapek, M. Hála, O. Zabeida, J. E. Klemberg-Sapieha, and L. Martinu, J. Appl. Phys. **111**, 023301 (2012).
[15] A. Aijaz, K. Sarakinos, D. Lundin, N. Brenning, and U Helmersson, Diamond Relat. Mater. **23**, 1 (2012).
[16] J. T. Gudmundsson, N. Brenning, D. Lundin, and U. Helmersson, J. Vac. Sci. Technol. A **30**, 030801 (2012).
[17] G. Clarke, A. Mishra, P. J. Kelly, and J. W. Bradley, Plasma Process. Polym. **6**, S548 (2009).
[18] F. Magnus, O. B. Sveinsson, S. Olafsson, and J. T. Gudmundsson, J. Appl. Phys. **110**, 083306 (2011).
[19] M. A. Liberman and A. J. Lichtenberg (John Wiley & Sons, Inc., New York, 1994), pp. 46–77.
[20] L. Poucques, J.C. Imbert, C. Boisse-Laporte, J. Bretagne, M. Ganciu, L. Teul-Gay, and M. Touzeau, Czech. J. Phys. **56**, B1301 (2006).
[21] H. Winter, F. Aumayr, and G. Lakits, Nucl. Instr. and Meth. in Phys. Res. B **182**, 15 (2001).
[22] A. Anders, Appl. Phys. Lett. **92**, 201501 (2008).
[23] C. Vitelaru, D. Lundin, G. D. Stancu, N. Brenning, J. Bretagne, and T. Minea, Plasma Sources Sci. Technol. **21**, 025010 (2012).

[24] A. Anders, S. Anders, M. A. Gundersen, and A. M. Martsinovskii, IEEE Trans. on Plasma Sci. **23**, 275 (1995).
[25] M. Hala, N. Viau, O. Zabeida, J. E. Klemberg-Sapieha, and L. Martinu, J. Appl. Phys. **107**, 043305 (2010).
[26] G. Y. Yushkov and A. Anders, J. Appl. Phys. **105**, 043303 (2009).
[27] J. Andersson, A. P. Ehiasarian, and A. Anders, Appl. Phys. Lett. **93**, 071504 (2008).
[28] J. Vlček and K. Burcalová, Plasma Sources Sci. Technol. **19**, 065010 (2010).
[29] J. Andersson and A. Anders, Phys. Rev. Lett. **102**, 045003 (2009).
[30] M. Hala, J. Capek, O. Zabeida, J. E. Klemberg-Sapieha, and L. Martinu, J. Phys. D: Appl. Phys. **45**, 055204 (2012).
[31] M. Audronis and V. Bellido-Gonzalez, Surf. Coat. Technol. **205**, 3613 (2011).